Theoretical Investigation on the Stability of Ionic Formic Acid Clusters

Leonardo Baptista,*,† Diana P. P. Andrade,† Alexandre Braga Rocha,† Maria Luiza M. Rocco,† Heloisa Maria Boechat-Roberty,‡ Enio F. da Silveira,§ Edílson Clemente da Silva,† and Graciela Arbilla†

Universidade Federal do Rio de Janeiro, Instituto de Química, Departamento de Físico-Química, Cidade Universitária, Ilha do Fundão, 21949-900, Rio de Janeiro, RJ, Brazil, Universidade Federal do Rio de Janeiro, Observatório do Valongo, Ladeira Pedro Antônio, 43, Centro, Rio de Janeiro, RJ, Brazil, and Pontifícia Universidade Católica do Rio de Janeiro, Departamento de Física, 22543-900, Rio de Janeiro, Brazil

Received: September 2, 2008; Revised Manuscript Received: October 3, 2008

Recent experimental results on positive charged formic acid clusters generated by the impact of ^{252}Cf fission fragments (FF) on icy formic acid target are examined in this paper by quantum mechanical calculations. Structures for the clusters series, $(HCOOH)_nH^+$ and $(HCOOH)_nH_3O^+$, where $2 \leq n \leq 4$, are proposed based on ab initio electronic structure methods. Results show that cluster growth does not present a regular pattern of nucleation. A stability analysis was performed considering the commonly defined stability function, where E is the total electronic energy plus the zero point vibrational energy correction, including the BSSE correction. The stability analysis leads to a picture that is compatible with experimental observations, indicating a decay of the stability with the increase of cluster mass. Temporal behavior of the clusters was evaluated by Born−Oppenheimer molecular dynamics to check the mechanism that provides cluster stability. The evaluated temporal profiles indicate the importance of hydrogen atom migration between the formic acid moieties to maintain the stability of the structures.

Introduction

Formic acid, HCOOH, the simplest carboxylic acid, may be a key compound in the formation of biomolecules such as acetic acid (CH_3COOH) and glycine (NH_2CH_2COOH), which is the simplest amino acid, in the interstellar medium (ISM) and it has been observed in several astronomical sources such as comets,[1] condritic meteorites,[2] and dark molecular clouds[3] among other astrophysical objects. Formic acid has been observed in some massive star-forming regions such as Sagittarius B2 and Orion KL. The search for glycine has turned out to be extremely difficult. This simple amino acid has long been searched for in the interstellar medium but has not been unambiguously detected so far. Its recent "detection" claimed by Kuan et al.[4] has been persuasively rebutted by Snyder et al.[5] However, amino acids have been found in meteorites on Earth, and recently, the detection of amino acetonitrile in Sgr B2(N)[6] has been reported (Belloche et al.). Amino acetonitrile was proposed early on as a possible direct precursor of glycine in the interstellar medium[7] (e.g., Brown et al.). Since formic acid and glycine are model systems for larger and more complex amino acids and proteins, it is worth understanding their behavior under exposure to high-energy radiation.[8] Accordingly, photodissociation processes and their ionic fragment yields play an essential role in the understanding of interstellar chemistry evolution.

Several experimental studies of the photodissociation of formic acid in the gas phase have been performed by using photons in the vacuum ultraviolet (VUV) and X-ray region as the ionization agent.[9−11] Moreover, Pilling and co-workers[12] have performed a series of experimental studies in an attempt to simulate the interaction between electrons (energy range from 0.5 to 2 keV) and protons (0.128 to 2 MeV) from the solar wind with cometary gaseous organic molecules.[12] However, their results cannot explain the ice/gas abundance ratio of formic acid (ice/gas $\sim 10^4$) observed by Ehrenfreund et al.[13]

Boechat-Roberty et al.[14] have shown that HCOOH is almost completely destroyed by soft X-rays, which would explain the low abundance of HCOOH in the gas phase. They have suggested that the preferential path for glycine formation from formic acid may occur in the presence of ice. Andrade et al.[15] have performed experimental studies of formic acid using plasma desorption mass spectrometry (PDMS) in an attempt to simulate the effects produced by the interaction of energetic particles/cosmic rays with condensed (ice phase) interstellar and cometary organic molecules. The ice temperature was about 56 K. α-Particles ^{252}Cf fission fragments (FF), which are heavy atomic highly charged cations with masses around 60−100 u and energies of about 65 MeV, were used to induce positive and negative ion desorption from the icy HCOOH surface. One of the main consequences of the impact of energetic particles on icy surfaces is that they release a large number of molecular clusters. An example of the PDMS spectrum is shown in Figure 1. From this desorption yeld distribution, it can be noticed that the $(HCOOH)_nH^+$ cluster series is the most intense found in the spectrum of cations, exhibiting a typical behavior, i.e., exponential decay of intensities as clusters mass increases.

In this paper, structures for the cluster series, $(HCOOH)_nH^+$ and $(HCOOH)_nH_3O^+$, where $2 \leq n \leq 4$, are proposed based on ab initio electronic structure methods. The stability of the clusters $(HCOOH)_nH^+$ and $(HCOOH)_nH_3O^+$ was also studied by Born−Oppenheimer molecular dynamics, using density

* Corresponding author: Phone: +55-21-2562-7174. Fax: +55-21-2562-7265. E-mail: baptista@iq.ufrj.br.
† Universidade Federal do Rio de Janeiro, Instituto de Química, Departamento de Físico-Química, Cidade Universitária.
‡ Universidade Federal do Rio de Janeiro, Observatório do Valongo.
§ Pontifícia Universidade Católica do Rio de Janeiro.

10.1021/jp807792s CCC: $40.75
Published on Web 11/21/2008

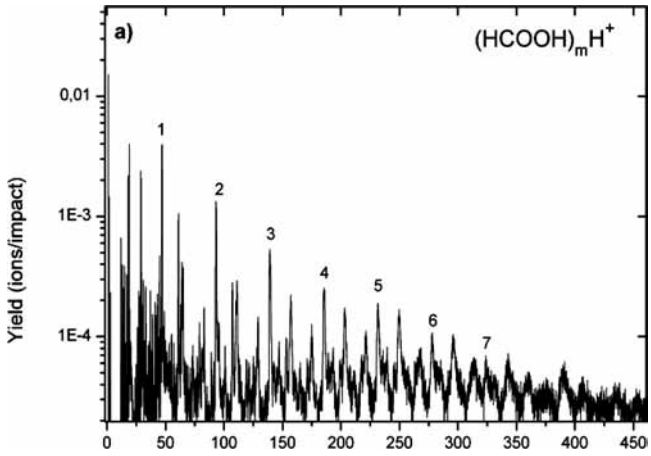

Figure 1. PDMS spectra of $(HCOOH)_mH^+$ cluster, $4 \leq m \leq 9$, modified from ref 11.

functional methods (DFT) in order to check the mechanism responsible for the stability of ionic clusters.

Computational Details

This study is divided in two main parts. The first includes a static approach to study the ionic formic acid clusters. The $(HCOOH)_nX^+$ series were studied, where $1 \leq n \leq 4$ and X^+ represents H^+ and H_3O^+. All geometries were fully optimized without any geometry constraint at the MP2 level with 6-311G(d,p) and 6-31+G(d,p) basis set. The structures were characterized as minima on the potential energy surface (PES) through harmonic frequency analysis.

The optimization procedures started by considering the most stable conformer of dimer, trimer, and tetramer already described in the literature[16] as geometry input. The ionic clusters were obtained by adding an ion in an arbitrary position of the neutral cluster and relaxing the structure until a minimum energy conformation was found. The ion optimizations were performed starting from several estimated structures to search for different conformers. Ionic clusters with positive formation energy (ΔE, ΔE_0) were dismissed.

The basis sets were chosen to account for the description of hydrogen bonding interactions present in the clusters and to avoid the basis set superposition error, which is present in a smaller basis.[17]

The binding energy (ΔE_b) for $(HCOOH)_nH^+$ and $(HCOOH)_nH_3O^+$ series, where $1 \leq n \leq 3$, was evaluated following the scheme proposed by Fernandez-Lima et al.,[18] and is shown in eq 1:

$$2(HCOOH)_nX^+ \rightarrow (HCOOH)_{n-1}X^+ + (HCOOH)_{n+1}X^+$$
$$\Delta E_b = E_{n-1} + E_{n+1} - 2E_n \quad (1)$$

where E is the electronic energy of the cluster, corrected by the zero point vibrational energy. The binding energy provides the stability of any cluster on growing or decreasing by one unit. This energy difference may be related to the stability of the cluster and the probability to reach the mass spectrometer detector with these structures.

The second part of this work is a Born−Oppenheimer molecular dynamics study. It was performed to investigate the mechanism that maintains the ionic clusters bonded. In these calculations, the PBE1PBE density function with 6-311G(d,p) basis set was used. According to Truhlar et al. this functional leads to a good description of weak interactions, such as hydrogen bond and interactions presented in charge transfer complexes, and correctly describes the asymptotic limit behavior.[19,20]

In a recent paper, Andersen and Carter,[21] studying the combustion of dimethyl ether, replaced all light hydrogen atoms in their system with deuterium atoms to minimize error in the dynamics caused by the complete neglect of quantum effects of light hydrogen. In the present study there is no interest in evaluating any dynamic property during the simulation, since the main goal is to analyze the structural changes of ionic clusters along the temporal evolution of the system and to verify the mechanism that stabilizes formic acid unities.

The initial conditions of the simulation were obtained from the electronic structure calculations. The input geometry was obtained at the MP2/6-311G(d,p) level. The Hessians were evaluated during the dynamics and the vibrational energy was obtained by thermal sampling.[22]

About ten simulations for the $(HCOOH)_2H^+$ cluster were performed. The first simulations were performed at 56 and 300 K with 85 fs of duration. Next, some dynamics were accomplished by transferring an excess energy to hydrogen atom numbers 8 and 11, corresponding to velocities up to 4.92×10^{14} bohr s^{-1} in order to check whether the hydrogen motion between the formic acid unities is involved in the stabilization of the clusters. These trajectories were evaluated at 56 K with trajectory time varying from 71 to 370 fs. The excess energy as well as the direction of the initial velocity vector was tested for both hydrogen atoms. First, an excess energy was added to one hydrogen atom and the direction of the velocity vector was tested. Next, an excess energy was added to two hydrogen atoms simultaneously and the direction of velocity vector of both atoms was tested. The simulation of $(HCOOH)_3H^+$ and $(HCOOH)_3H_3O^+$ clusters proceeded at 56 and 300 K with trajectory time varying from 360 to 760 fs.

Results and Discussion

The optimized geometries of neutral and ionic clusters are shown in Figures 2−4 and the geometric parameters are listed in Tables 1−3. The results show a distortion of the geometries of ionic clusters relative to the neutral ones. The cluster growth does not present a regular pattern of nucleation, such as observed in other processes, as the growth of $NH_4^+(NH_3)_n$ clusters.[18,23] In that case, the NH_4^+ is solvated by NH_3 molecules and shows an organized structure, which is not observed in the ionic formic acid clusters.

The $(HCOOH)_nH^+$ series has one additional hydrogen added to the carboxyl group. The dimer structure is distorted from the neutral dimer geometry and has the shortest hydrogen bonding distance, $r(O_4H_{11})$. The neutral dimer presents two equivalent hydrogen bonds, with a bond distance of 1.711 Å, while the ionic cluster presents one oxygen atom interacting simultaneously with two hydrogens of the protonated formic acid. Qualitatively, the neutral and ionic trimers show the same structure. The three unities of formic acid lie in the same plane, having the hydrogen added to one carboxyl group. The tetramer geometry corresponds to the interaction between one ionic formic acid dimer and a neutral formic acid dimer (Figure 4).

The $(HCOOH)_nH_3O^+$ series is mainly formed by a protonated formic acid cluster associated with a water molecule. The dimer has a short hydrogen bond distance, $r(O_7H_9) = 1.393$ Å, but qualitatively has a structure similar to the neutral dimer. Two different conformations were obtained for the trimer, described as a protonated formic acid trimer associated with a water molecule. The first trimer conformation, presented in Figure 3c,

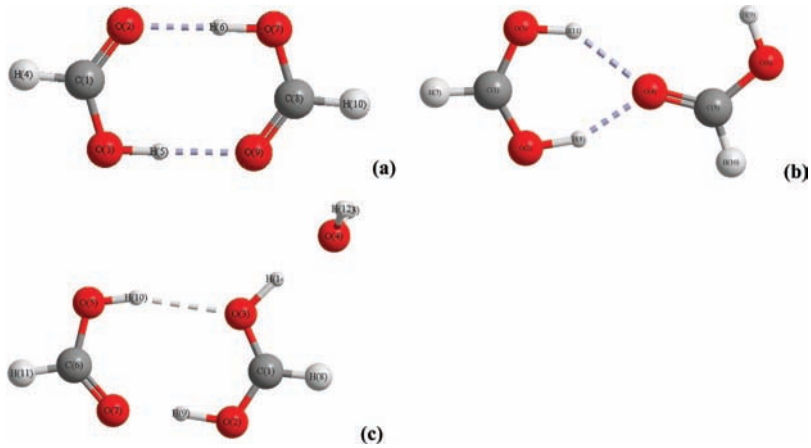

Figure 2. Optimized geometries of formic acid dimer at MP2/6-311G**: (a) neutral formic acid dimer; (b) $(HCOOH)_2H^+$ cluster; (c) $(HCOOH)_2H_3O^+$ cluster.

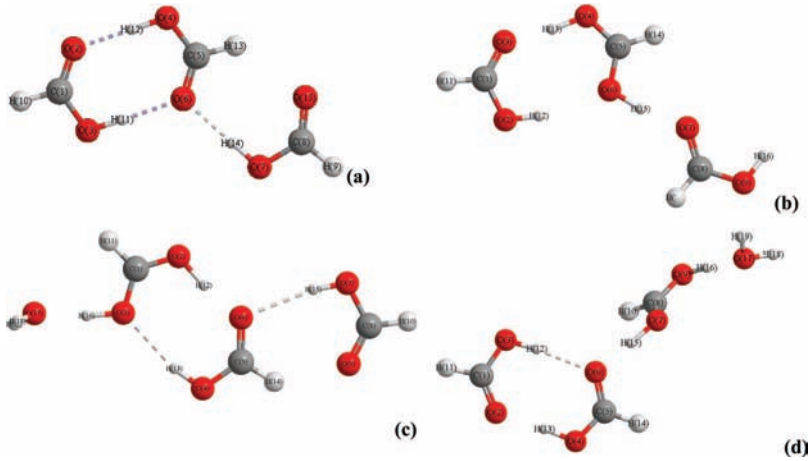

Figure 3. Optimized geometries of formic acid trimer at MP2/6-311G**: (a) neutral formic acid trimer; (b) $(HCOOH)_3H^+$ cluster; (c) first conformation of $(HCOOH)_3H_3O^+$ cluster; (d) second conformation of $(HCOOH)_3H_3O^+$ cluster.

TABLE 1: Geometric Parameters of Formic Acid Dimmers Evaluated at the MP2/6-311G(d,p) Level[a]

$(HCOOH)_2$		$(HCOOH)_2H^+$		$(HCOOH)_2H_3O^+$	
$r(O_2H_6)$	1.711	$r(O_4H_8)$	1.853	$r(O_7H_9)$	1.393
$r(O_9H_5)$	1.711	$r(O_4H_{11})$	1.607	$r(O_3H_{10})$	2.180
$r(C_1C_8)$	3.821	$r(C_1C_5)$	4.168	$r(C_1C_6)$	3.934
$\theta(H_{11}O_6C_5)$	126.46	$\theta(C_5O_4H_{11})$	156.16	$\theta(H_{10}O_3C_1)$	122.44
$\theta(O_2C_1O_3)$	126.60	$\theta(O_2C_1O_3)$	126.01	$\theta(O_2C_1O_3)$	122.69
$\psi(C_5O_6H_{11}O_3)$	2.66	$\psi(O_6C_5O_4H_{11})$	0.37	$\psi(C_1O_3H_{10}O_5)$	−0.14

[a] All bond distances are in angstroms, bond angles and dihedral angles are in degrees.

is similar to the $(HCOOH)_2H_3O^+$ cluster, with an additional formic acid molecule. This geometry shows a short hydrogen bond, $r(O_6H_{12}) = 1.377$ Å, and a stretching of 25% over the $r(O_3H_{13})$ distance relative to the $r(O_2H_{12})$ distance of the neutral cluster (Figure 2a and 2c). The second conformation, Figure 3d, presents a formic acid moiety bending out of the plane containing the dimer structure, due to the presence of the water molecule. As observed previously, the hydrogen bonds that stabilize the trimer were modified. By comparing the neutral trimer with the $(HCOOH)_3H_3O^+$ cluster it may be seen the $r(O_2H_{13})$ distance is shortened by 8% relative to the $r(O_2H_{12})$ distance, the $r(O_6H_{12})$ distance is stretched by 10% relative to the $r(O_6H_{11})$ distance, and the $r(O_6H_{15})$ distance is shortened by 23% relative to the $r(O_6H_{14})$ distance.

The ionic tetramer is formed by a dimer interacting with a protonated formic acid plus another formic acid molecule. If the formic acid tetramer is considered as two unities of formic acid dimers, as can be seen in Table 3 and in Figure 4, the inclusion of the water molecule plus the proton distorts one dimeric structure. New hydrogen bonds between the formic acid molecules were formed: oxygen 4 interacts with hydrogen 13 and hydrogen 22 of the water molecule; hydrogen 14 interacts with oxygen 9.

Next, the binding energies were evaluated for the clusters $(HCOOH)_nH^+$ and $(HCOOH)_nH_3O^+$ from $n = 1-3$. The binding energy corresponds to the electronic nucleation energy with the minus sign, ΔE_b.[23a] In this paper, this energy was defined by the following process:[18]

$$2(HCOOH)_nX^{\pm} \rightarrow (HCOOH)_{n-1}X^{\pm} + (HCOOH)_{n+1}X^{\pm}$$

$$\Delta E_b = E_{n-1} + E_{n+1} - 2E_n$$

It corresponds to the energy change resulting from the encounter of two clusters of the same order leading to new clusters with a different number of formic acid unities. The basis set superposition error was considered in the evaluation of the binding energy.

Experimentally, the PDMS spectrum shows the cluster ion abundance decreasing exponentially as the number of formic acid molecules increases. The peaks of high intensity correspond to the clusters with low molecular weight, except for the anomalous $(HCOOH)_nOH^-$ series. Table 4 shows the ΔE_b evaluated for the clusters $(HCOOH)_nH^+$ and $(HCOOH)_nH_3O^+$

TABLE 2: Geometric Parameters of Formic Acid Trimers Evaluated at the MP2/6-311G(d,p) Level[a]

$(HCOOH)_3$		$(HCOOH)_3H^+$		$(HCOOH)_3H_3O^+$ (1)		$(HCOOH)_3H_3O^+$ (2)	
$r(O_2H_{12})$	1.692	$r(O_3H_{13})$	1.414	$r(O_3H_{13})$	2.113	$r(O_2H_{13})$	1.550
$r(O_6H_{11})$	1.748	$r(O_6H_{12})$	2.162	$r(O_6H_{12})$	1.377	$r(O_6H_{12})$	1.919
$r(O_6H_{14})$	1.814	$r(O_6H_{15})$	1.041	$r(O_6H_{15})$	2.177	$r(O_6H_{15})$	1.398
$r(C_1C_5)$	3.846	$r(C_1C_5)$	3.934	$r(C_1C_5)$	3.921	$r(C_1C_5)$	3.871
$\theta(H_{11}O_6C_5)$	126.20	$\theta(H_{12}O_6C_5)$	122.42	$\theta(H_{12}O_6C_5)$	130.75	$\theta(H_{12}O_6C_5)$	122.23
$\theta(O_2C_1O_3)$	126.40	$\theta(O_2C_1O_3)$	126.04	$\theta(O_2C_1O_3)$	122.58	$\theta(O_2C_1O_3)$	125.49
$\psi(C_5O_6H_{11}O_3)$	0.85	$\psi(C_5O_6H_{12}O_2)$	0.34	$\psi(C_5O_6H_{12}O_2)$	−179.61	$\psi(C_5O_6H_{12}O_3)$	−172.87

[a] All bond distances are in angstroms, bond angles and dihedral angles are in degrees.

TABLE 3: Geometric Parameters of Formic Acid Tetramers Evaluated at the MP2/6-311G(d,p) Level[a]

$(HCOOH)_4$		$(HCOOH)_4H^+$		$(HCOOH)_4H_3O^+$	
$r(O_4H_7)$	1.713	$r(O_7H_{21})$	1.393	$r(O_4H_{13})$	1.608
$r(O_3H_8)$	1.713	$r(O_3H_{18})$	1.598	$r(O_9H_{14})$	1.671
$r(O_{13}H_{18})$	1.713	$r(O_2H_{14})$	1.735	$r(O_9H_{18})$	1.750
$r(O_{14}H_{17})$	1.713	$r(O_{10}H_{13})$	1.619	$r(O_{10}H_{17})$	1.692
$r(C_1C_2)$	3.825	$r(C_5C_8)$	4.297	$r(C_1C_5)$	4.510
$r(C_{11}C_{12})$	3.825	$r(C_1C_{11})$	3.806	$r(C_7C_{11})$	3.859
$\theta(C_1C_2C_{12})$	78.83	$\theta(C_5C_8C_{11})$	88.95	$\theta(C_5C_1C_{11})$	78.12
$\theta(O_3C_1O_5)$	126.47	$\theta(O_6C_5O_4)$	128.63	$\theta(O_2C_1O_3)$	128.43
$\psi(C_1C_2C_{12}C_{11})$	−43.89	$\psi(C_5C_8C_{11}C_1)$	55.29	$\psi(C_5C_1C_{11}C_7)$	49.21

[a] All bond distances are in angstroms, bond angles and dihedral angles are in degrees.

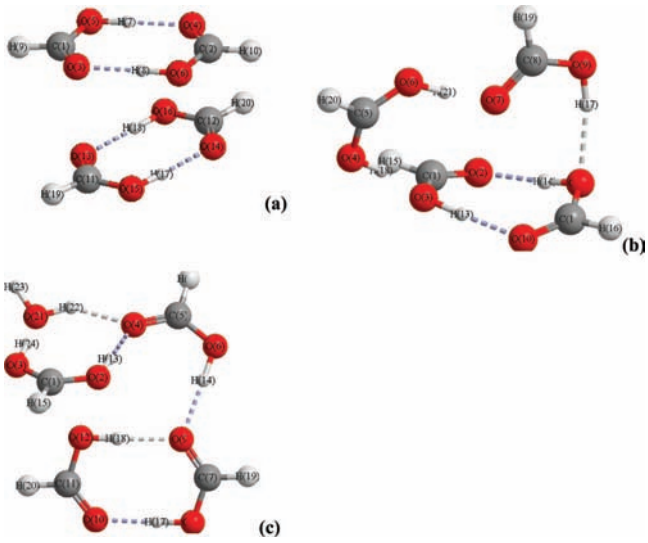

Figure 4. Optimized geometries of formic acid tetramer at MP2/6-311G**: (a) neutral formic acid tetramer; (b) $(HCOOH)_4H^+$ cluster; (c) $(HCOOH)_4H_3O^+$ cluster.

TABLE 4: Binding Energy for $(HCOOH)_nH^+$ and $(HCOOH)_nH_3O^+$ Clusters, Where $1 \leq n \leq 3$, at the MP2/6-31+G(d,p) Level[a]

	energy binding	
n	$(HCOOH)_nH^+$	$(HCOOH)_nH_3O^+$
1	140.53	19.50
2	10.57	10.22
3	13.80	−12.57

[a] Values in kcal mol^{-1}.

and, as it can be seen, qualitatively the values represent the experimental behavior. It is important to note that the negative value in Table 4 does not mean that the $(HCOOH)_3H_3O^+$ cluster is unbound, but indicates that the cluster may rearrange more easily than smaller clusters. These facts indicate that the stability of clusters decreases with increasing molecular weight. In fact, the most abundant ion of the $(HCOOH)_nH^+$ series is the $(HCOOH)H^+$ species, with ΔE_b one order of magnitude superior to the binding energy of the $(HCOOH)_2H^+$ cluster.

To check the mechanism that provides the stability of ionic clusters, temporal behavior of ionic clusters was simulated by Born−Oppenheimer molecular dynamics. The animated trajectory may be seen in the Supporting Information.

Initially, simulations were performed for the $(HCOOH)_2H^+$ cluster to analyze the role of the additional hydrogen in the stability of the cluster. The simulations of the $(HCOOH)_2H^+$ cluster, at experimental and room temperatures, 56 and 300 K, respectively (simulations at 300 K were included in the Supporting Information), show that a cluster is stable on the course of simulation, without any bond cleavage and loss of the dimeric structure. It is quite possible that, after collision with ^{252}Cf fragments, this cluster is formed in a vibrationally excited state. Hence, the authors decided to investigate whether the stability of the cluster would be kept under this condition. The idea was to investigate whether the transfer of the proton between moieties could stabilize the cluster. This was accomplished by adding an excess of energy to hydrogen atoms 8 and 11 separately, and then an excess energy was added to both hydrogen atoms. In the first case, the excess energy leads to hydrogen migration between the formic acids, as observed in Figure 5. This migration maintains the stable structure and avoids the breaking of the dimeric structure into energies corresponding to proton velocities of up to 4.92×10^{14} bohr s^{-1}. For velocities greater than that the structure breaks down. In the snapshots depicted in Figures 5−7 it is possible to see the rotation of both molecules in the cluster to maximize the interaction between the two moieties. The clusters remain stable during the course of simulation.

The clusters break into a neutral and a protonated formic acid when an excess energy is simultaneously added to both hydrogen atoms. This behavior is observed in all cases as can be seen in the snapshots (Figure 8) for the $(HCOOH)_2H^+$ cluster. Initially, these atoms oscillate between the formic acid unities, but the excess energy on the hydrogen atoms pulls the formic acid molecules apart.

To check whether the hydrogen migration is important to the high order clusters and to other clusters such as that in the $(HCOOH)_nH_3O^+$ series, temporal behavior of $(HCOOH)_2H_3O^+$, $(HCOOH)_3H^+$, and $(HCOOH)_3H_3O^+$ clusters was simulated at 56 and 300 K.

The dynamic evolution of the $(HCOOH)_2H_3O^+$ cluster is shown in the Supporting Information. It can be seen from the snapshots that the hydrogen presents a labile character, compared with the $(HCOOH)_2H^+$ cluster, since a hydrogen migration was observed in 46 fs at 300 K. The cluster maintains the dimeric structure and a water molecule associated to it during the simulation. The temporal behavior of hydrogen 14 indicates that the cluster is formed by a protonated formic acid dimer with a water molecule. Again, it is possible to see that the clusters are stable due to the

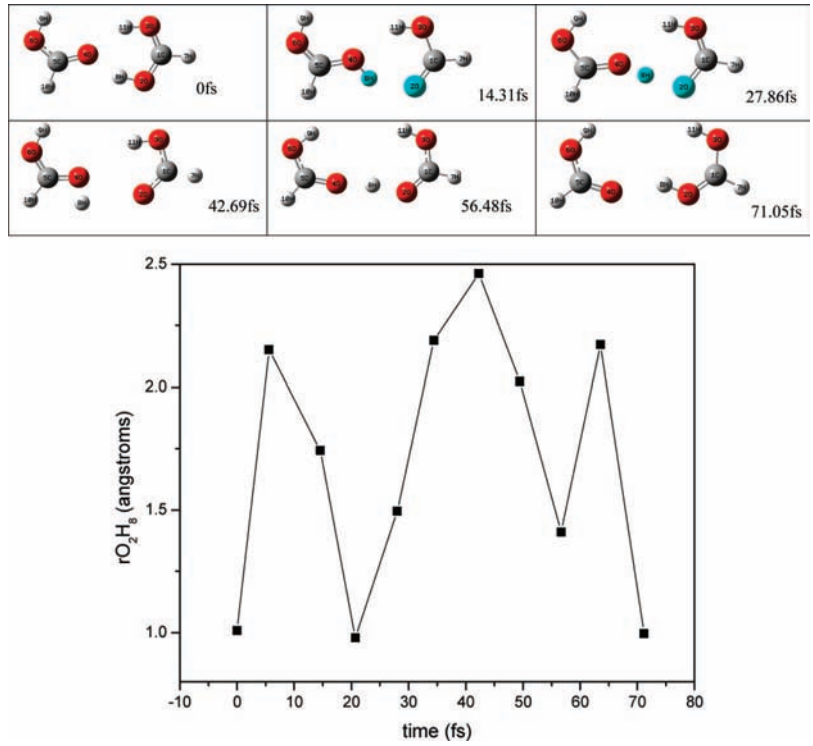

Figure 5. Snapshots of $(HCOOH)_2H^+$ cluster during the simulation at 56 K. Bottom: Changing of $r(H_2O_8)$ bond distance on the course of simulation (PBE1PBE/6-311G(d,p)).

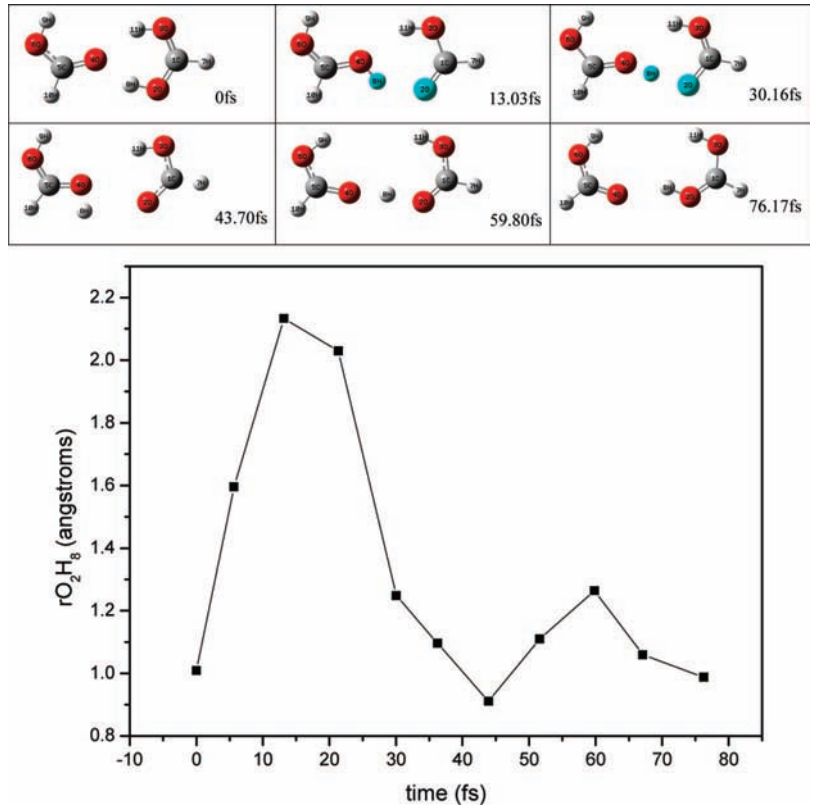

Figure 6. Snapshots of $(HCOOH)_2H^+$ cluster during the simulation at 56 K. Bottom: Changing of $r(H_2O_8)$ bond distance on the course of simulation (PBE1PBE/6-311G(d,p)).

hydrogen migration between the formic acid unities and a hydrogen bond between hydrogen 14 and oxygen 4.

The hydrogen migration plays an important role in the stabilization of the $(HCOOH)_3H^+$ cluster. As in the preceding case, hydrogen atoms 13 and 15 are labile and move from the central formic acid to the other formic acid unities. During the simulation, the $r(O_4H_{13})$ and $r(O_7H_{15})$ bond distances have an average value longer than the usual r(OH) distance, 1.178 Å for the $r(O_4H_{13})$ bond distance and 1.390 for the $r(O_7H_{15})$ bond distance. This stretching was due to the interaction with the oxygen of neighboring formic acid and the oscillation of the hydrogen between two different formic acid molecules (Figure 9).

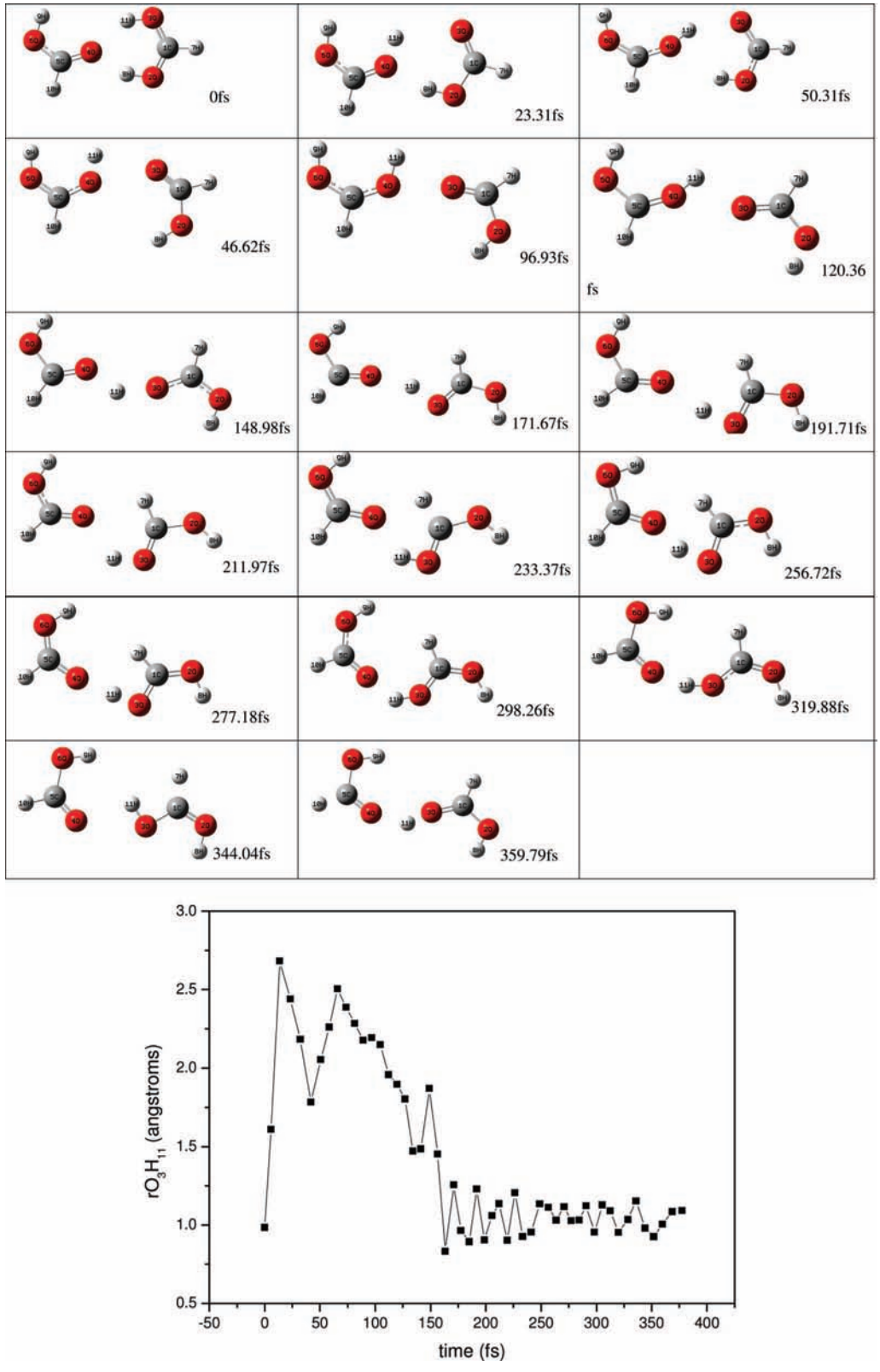

Figure 7. Snapshots of $(HCOOH)_2H^+$ cluster during the simulation at 56 K. Bottom: Changing of $r(H_3O_{11})$ bond distance on the course of simulation (PBE1PBE/6-311G(d,p)).

According to Figure 3, two different conformations for the $(HCOOH)_3H_3O^+$ cluster were obtained, relative to the orientation of the H_3O^+ ion. The dynamics for both conformations (Figures 10 and 11) confirms that the clusters are formed mainly by a protonated formic acid trimer plus a water molecule bonded to the cluster by a hydrogen bond. The first conformation (Figure 3c) breaks along the dynamics in 550 fs (Figure 10), leading to a formic acid molecule and the $(HCOOH)_2H_3O^+$ cluster. However, the second conformation, Figure 3b, is stable along the entire dynamics (Figure 11). By comparing Figures 10 and 11 it is possible to see that the hydrogen atom migration plays an important role in maintaining the stability of the clusters. In Figure 10, the formic acid molecule dissociates, since hydrogen 15 does

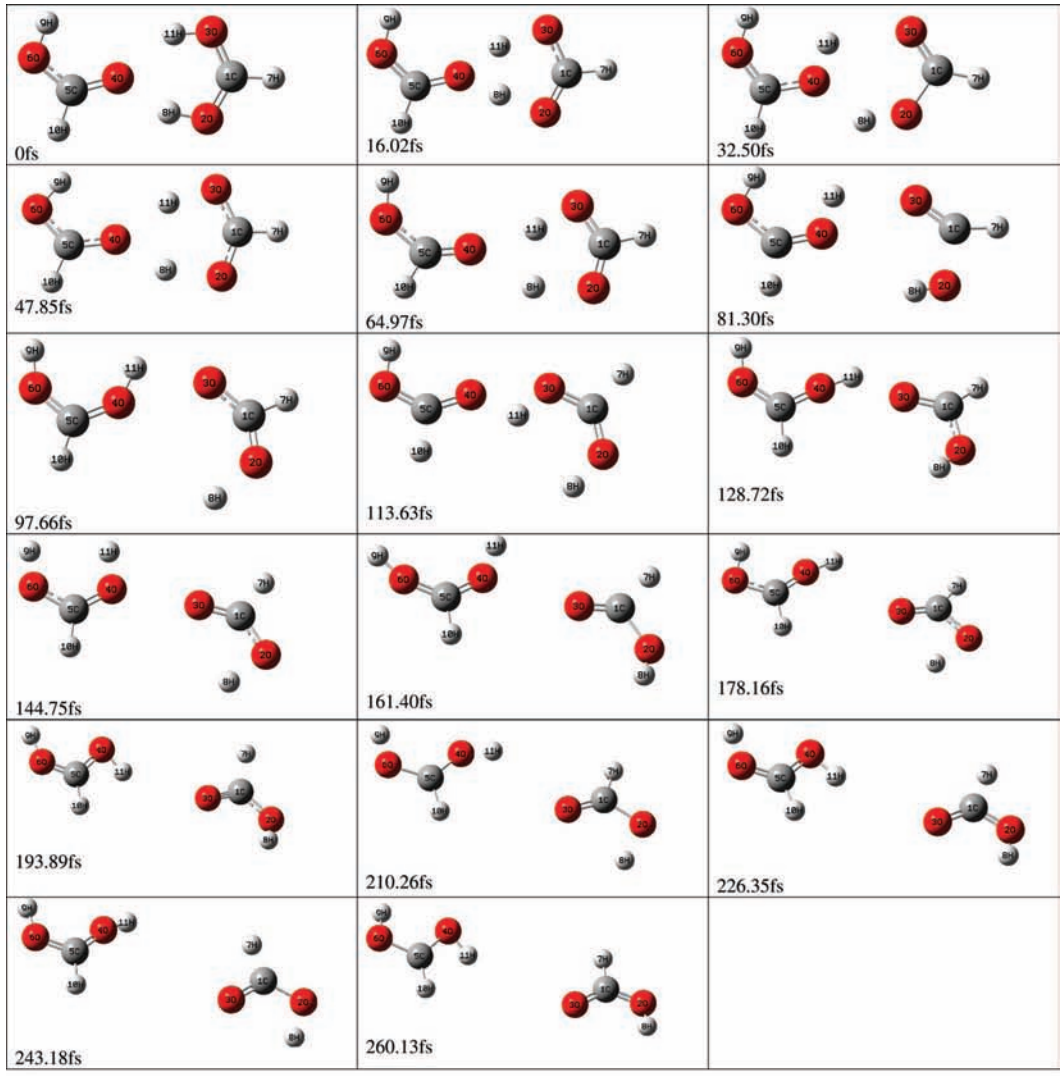

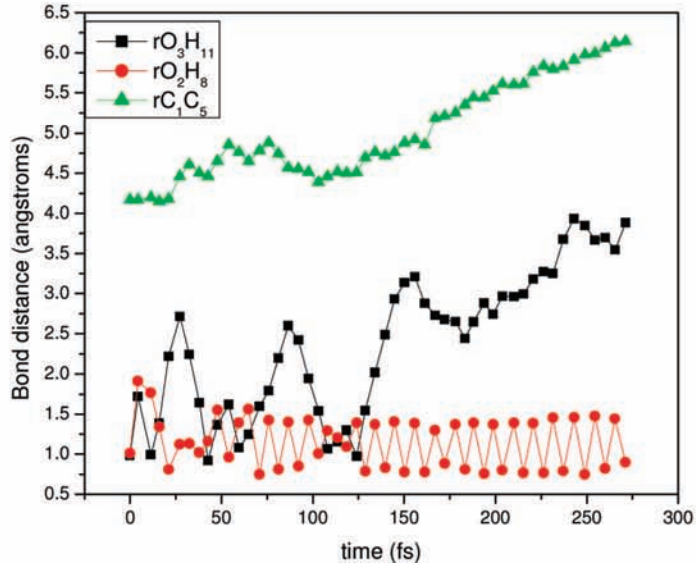

Figure 8. Snapshots of $(HCOOH)_2H^+$ cluster during the simulation at 56 K. Bottom: Changing of $r(H_3O_{11})$, $r(H_2O_8)$, and $r(C_1C_5)$ bond distances on the course of simulation (PBE1PBE/6-311G(d,p)).

not move between the formic acid moieties, while in Figure 11, the formic acid cluster is stable due to the migration of hydrogens 13 and 15 between the formic acid moieties.

From Figures 3, 10, and 11 it is possible to predict that the correct assignment of the $(HCOOH)_nH_3O^+$ series is $(HCOOH)_n(H^+)(H_2O)$, since the optimized geometries and the Born−Oppenheimer dynamics show a protonated formic acid cluster associated to one water molecule as minima on the potential energy surface and a stable structure during the dynamic calculation.

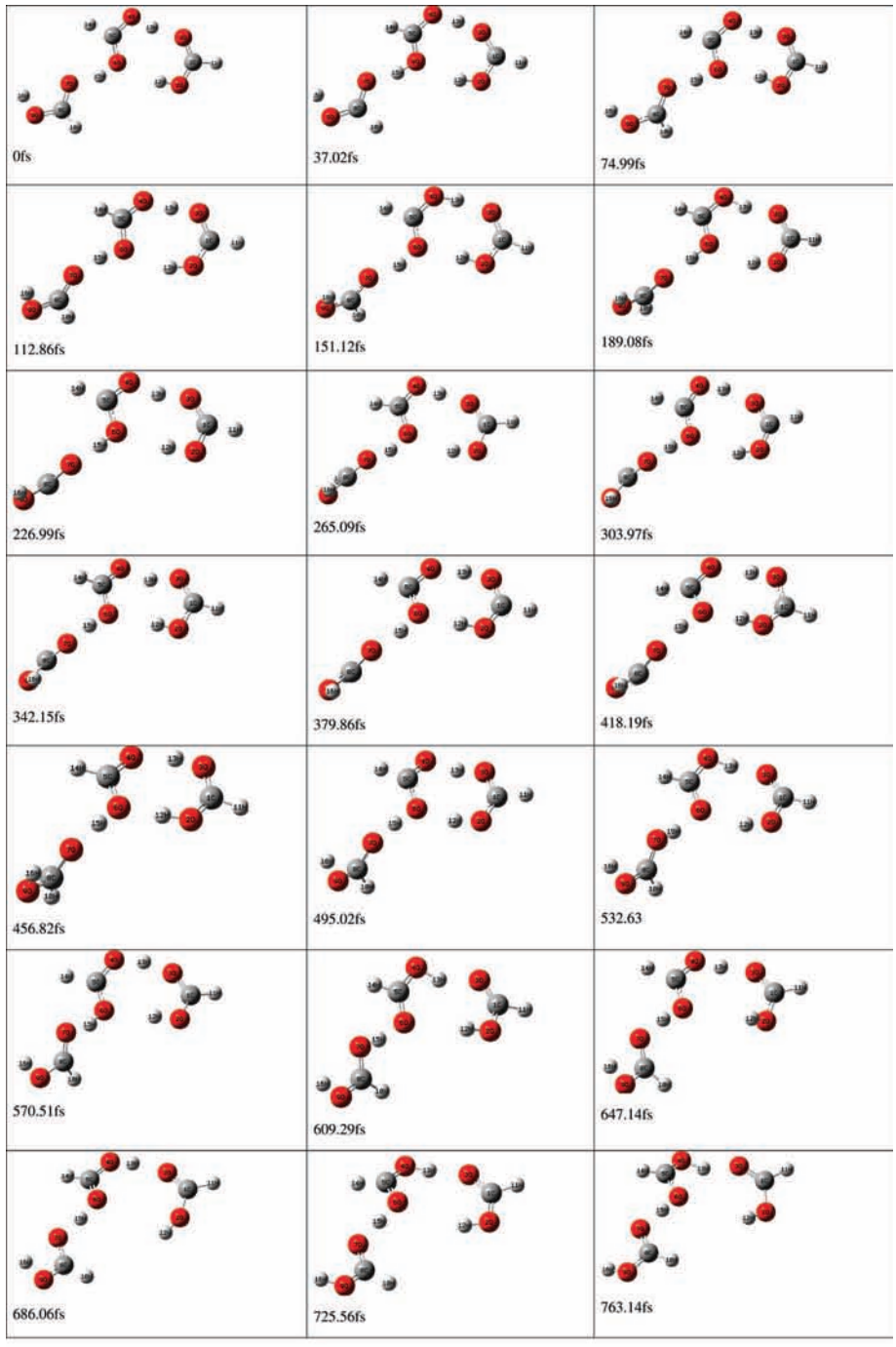

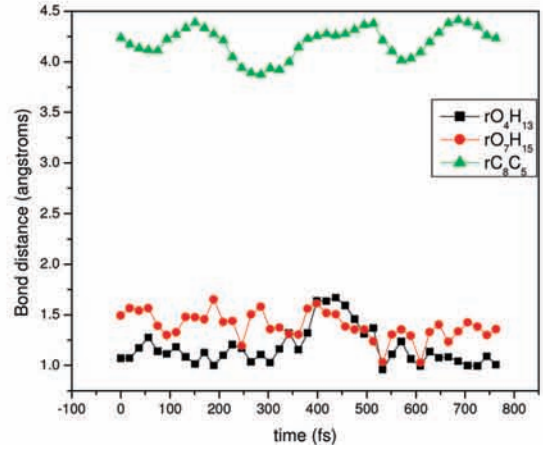

Figure 9. Snapshots of $(HCOOH)_3H^+$ cluster during the simulation at 56 K. Bottom: Changing of $r(H_4O_{13})$, $r(H_7O_{15})$, and $r(C_8C_5)$ bond distances on the course of simulation (PBE1PBE/6-311G(d,p)).

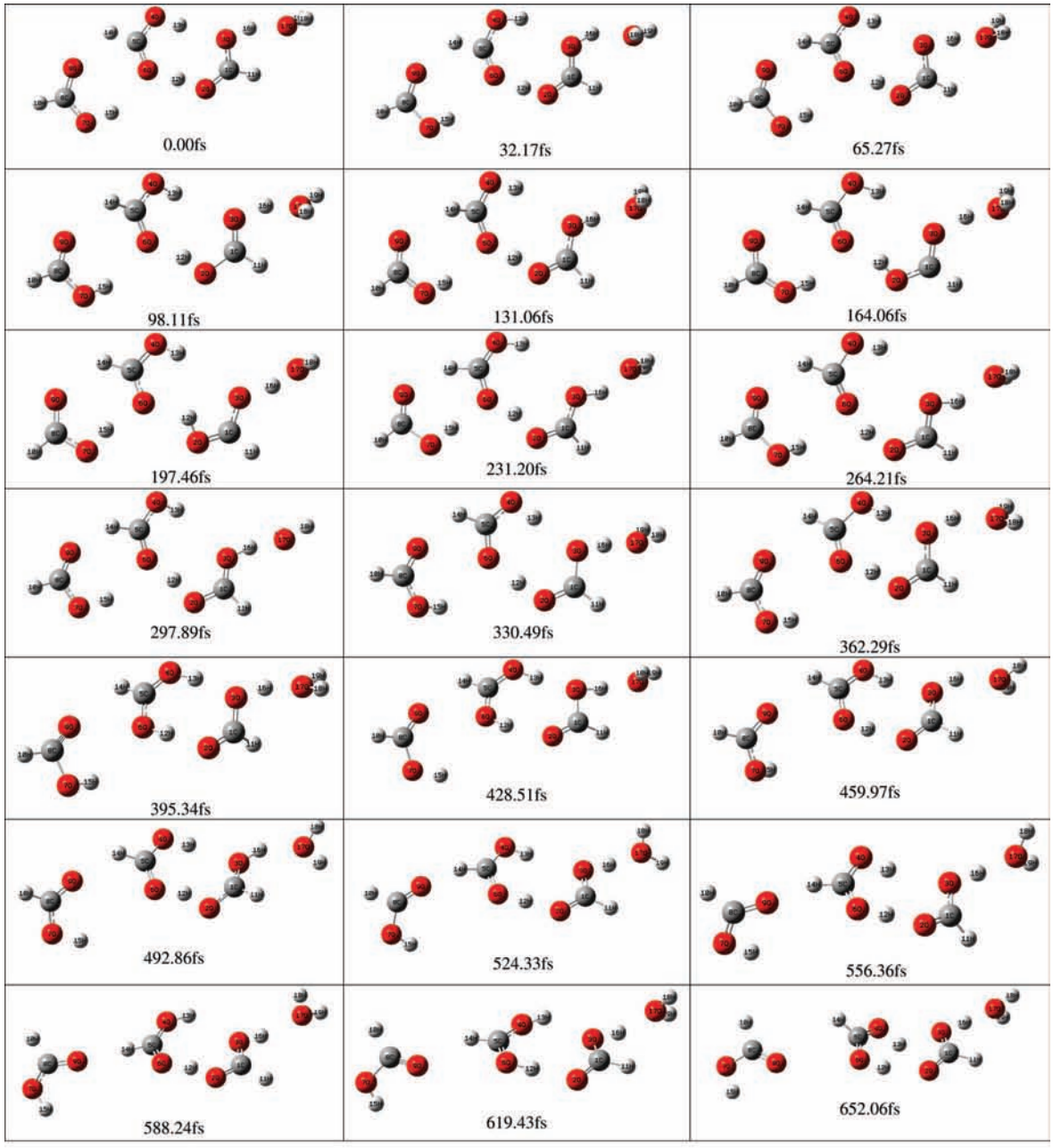

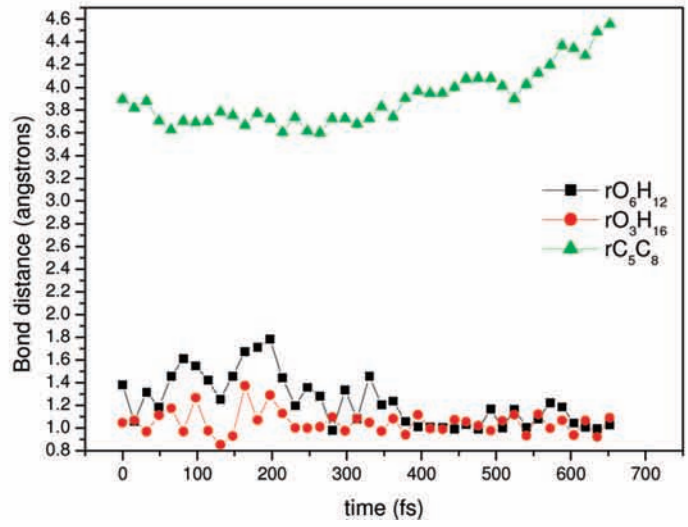

Figure 10. Snapshots of $(HCOOH)_3H_3O^+$ cluster, conformation (1), during the simulation at 300 K. Bottom: Changing of $r(O_6H_{12})$, $r(O_3H_{16})$, and $r(C_5C_8)$ bond distances on the course of simulation (PBE1PBE/6-311G(d,p)).

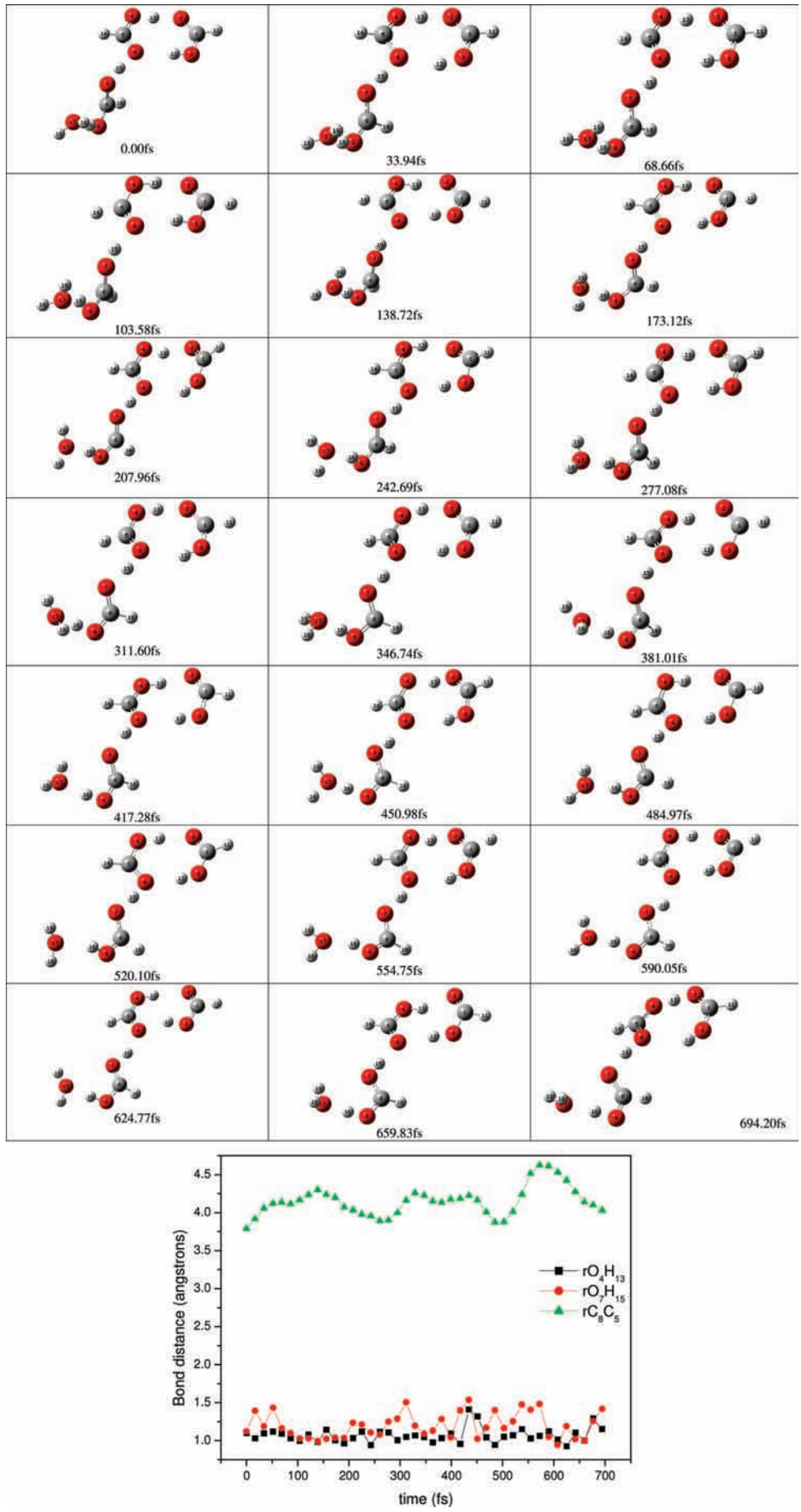

Figure 11. Snapshots of $(HCOOH)_3H_3O^+$ cluster, conformation (2), during the simulation at 56 K. Bottom: Changing of $r(O_6H_{12})$, $r(O_3H_{16})$, and $r(C_5C_8)$ bond distances on the course of simulation (PBE1PBE/6-311G(d,p)).

Conclusions

Positively charged formic acid clusters generated by the impact of ^{252}Cf fission fragments (FF) on icy formic acid target have been studied by quantum mechanical calculations. The combination of time-independent calculations with the Born−Oppenheimer molecular dynamics provides the correct assignment of the structures of the clusters formed in the PDMS spectra.

The $(HCOOH)_nH^+$ series presents an additional hydrogen added to one carboxyl group that may oscillate between the formic acid moieties. The correct assignment of the $(HCOOH)_nH_3O^+$ series is $(HCOOH)_n(H^+)(H_2O)$, since the optimized geometries and the Born−Oppenheimer dynamics show a protonated formic acid cluster associated to one water molecule as minima on the potential energy surface and a stable structure during the dynamic calculation.

Additionally, the Born−Oppenheimer dynamics suggests that the hydrogen migration between the formic acid unities plays an important role in maintaining the ionic cluster stability. If the formed dimer is vibrationally excited, one hydrogen atom may translate in the cluster structure without loss of the dimeric structure.

The stability analysis provides an additional insight about the cluster geometries, which indicates an exponential decay of the cluster stability with the mass increase, as observed in the experimental PDMS spectrum. In fact, the most abundant ion of the $(HCOOH)_nH^+$ series is the $(HCOOH)H^+$ species, with ΔE_b being one order of magnitude superior to the binding energy of the $(HCOOH)_2H^+$ cluster.

Acknowledgment. The authors thank CNPq, CAPES, and FAPERJ for financial support.

Supporting Information Available: The animated trajectory of all Born−Oppenheimer molecular dynamics. This material is available free of charge via the Internet at http://pubs.acs.org.

References and Notes

(1) (a) Crovisier, J.; Bockelée-Morvan, D. *Space Sci. Rev.* **1999**, *90*, 19. (b) Crovisier, J.; Bockelée-Morvan, D.; Colom, P.; Biver, N.; Despois, D.; Lis, D. C. *Astron. Astrophys.* **2004**, *418*, 1141.

(2) Briscoe, J. F.; Moore, C. B. *Meteoritics* **1993**, *28*, 330.

(3) Ehrenfreund, P. E.; Charnley, S. *Annu. Rev. Astron. Astrophys.* **2000**, *38*, 427.

(4) Kuan, Y.-J.; Charnley, S. B.; Huang, H.-C.; Tseng, W.-L.; Kisiel, Z. *Astrophys. J.* **2003**, *593*, 848.

(5) Snyder, L. E.; Lovas, F. J.; Hollis, J. M.; Friedel, D. N. *Astrophys. J.* **2005**, *619*, 914.

(6) Belloche, A.; Menten, K. M.; Comito, C.; Müller, H. S. P.; Schilke, P.; Ott, J.; Thorwirth, S.; Hieret, C. *Astron. Astrophys.* **2008**, *482*, 179B.

(7) Brown, R. D.; Godfrey, P. D.; Ottrey, A. L.; Storey, J. W. V. *J. Mol. Spectrosc.* **1977**, *68*, 359.

(8) Pelc, A.; Sailer, W.; Scheier, P.; Probst, M.; Mason, N. J.; Illenberger, E.; Märk, T. D. *Chem. Phys. Lett.* **2002**, *361*, 277.

(9) Leach, S.; Schwell, M.; Dulieu, F.; Chotin, J. L.; Jochimsb, H. W.; Baumgärtelb, H. *Phys. Chem. Chem. Phys.* **2002**, *4*, 5025.

(10) Sorrell, W. H. *Astrophys. J.* **2001**, *555*, 129.

(11) Su, H.; Yong, H.; Fanao, K. *J. Chem. Phys.* **1999**, *113*, 1891.

(12) Pilling, S.; Santos, A. C. F.; Wolff, W.; Sant'anna, M. M.; Barros, A. L. F.; de Souza, G. G. B.; de Castro Faria, N.; Boechat-Roberty, H. M. *Mon. Not. R. Astron. Soc.* **2006**, *372*, 1379.

(13) Ehrenfreund, P.; D'Hendecourt, L.; Charnley, S.; Ruiterkamp, R. *J. Geophys. Res.* **2001**, *106*, 33291.

(14) Boechat-Roberty, H. M.; Pilling, S.; Santos, A. C. F. *Astron. Astrophys.* **2005**, *438*, 915.

(15) (a) Andrade, D. P. P.; Rocco, M. L. M.; Boechat-Roberty, H. M.; Iza, P.; Martinez, R.; Homem, M. G. P.; da Silveira, E. F. *J. Electron Spectrosc. Relat. Phenom.* **2006**, *155*, 124. (b) Andrade, D. P. P.; Boechat-Roberty, H. M.; da Silveira, E. F.; Pilling, S.; Iza, P.; Martinez, R.; Farenzena, L. S.; Homem, M. G. P.; Rocco, M. L. M. *J. Phys. Chem. C* **2008**, *112*, 11954.

(16) (a) Rmón, J. M. H.; Ríos, M. A. *Chem. Phys.* **1999**, *250*, 155;(b) Roy, A. K.; Thakkar, A. J. *Chem. Phys. Lett.* **2004**, *386*, 162. (c) Roy, A. K.; Thakkar, A. J. *Chem. Phys. Lett.* **2004**, *393*, 347. (d) Zhao, Y.; Truhlar, D. G. *J. Phys. Chem. A* **2005**, *109*, 6624.

(17) Sílvia, S.; Miquel, D.; Dannenberg, J. J. *J. Chem. Phys.* **1996**, *105*, 11024.

(18) Fernandez-Lima, F. A.; Ponciano, C. R.; Nascimento, M. A. C.; da Silveira, E. F. *J. Phys. Chem. A* **2006**, *110*, 10018.

(19) (a) Zhao, Y.; Truhlar, D. G. *J. Chem. Theory Comput.* **2005**, *1*, 415. (b) Zhao, Y.; Truhlar, D. G. *J. Phys. Chem. A* **2004**, *108*, 6908. (c) Xin, X.; Goddard, W. A. *J. Phys. Chem. A* **2004**, *108*, 2305.

(20) Perdew, J. P.; Burke, K.; Ernzenhof, M. *Phys. Rev. Lett.* **1996**, *77*, 3865.

(21) Andersen, A.; Carter, E. *J. Phys. Chem. A* **2006**, *110*, 1393.

(22) (a) Helgaker, T.; Uggerud, E.; Jensen, H. J. A. *Chem. Phys. Lett.* **1990**, *173*, 145. (b) Chen, W.; Hase, W. L.; Schlegel, H. B. *Chem. Phys. Lett.* **1994**, *228*, 436. (c) Millam, J. M.; Bakken, V.; Chen, W.; Hase, W. L.; Schlegel, B. H. *J. Chem. Phys.* **1999**, *111*, 3800. (d) Li, X.; Millam, J. M.; Schlegel, B. H. *J. Chem. Phys.* **2000**, *113*, 10062.

(23) (a) Nakai, H.; Goto, T.; Ichikawa, T.; Okada, Y.; Orii, T.; Takeuchi, K. *Chem. Phys.* **2000**, *262*, 201. (b) Wanga, B.; Changa, J.; Jiangb, J.; Lin, S. *Chem. Phys.* **2002**, *276*, 93.

JP807792S